J|A|C|S
ARTICLES
Published on Web 03/08/2005

Viscosity of the Aqueous Liquid/Vapor Interfacial Region: 2D Electrochemical Measurements with a Piperidine Nitroxy Radical Probe

Deng Guo Wu, Andrew D. Malec, Martin Head-Gordon, and Marcin Majda*

Contribution from the Department of Chemistry, University of California, Berkeley, California 94720-1460

Received November 22, 2004; E-mail: majda@berkeley.edu

Abstract: Surface partitioning of 2,2,6,6-tetramethyl-1-piperidynyloxy radical (Tempo) to the air/water interface follows a Langmuir isotherm. The partition constant was obtained by the surface tension measurements in the concentration range of $1.0 \times 10^{-4}-2.4 \times 10^{-3}$ M yielding $K = 640 \pm 99$ M^{-1}. The lateral mobility of Tempo at the air/water interface was measured electrochemically in the surface concentration range of $2.0 \times 10^{-11}-1.4 \times 10^{-10}$ mol/cm^2, corresponding to ca. 7.3−50% full monolayer coverage. The measurements employed cyclic voltammetry with line microelectrodes touching the air/water interface. The Tempo lateral diffusion constant of $(1.5 \pm 0.7) \times 10^{-4}$ cm^2/s is independent of surface concentration below 4.0×10^{-11} mol/cm^2. The extent of Tempo water interactions was assessed by the electronic structure calculations. These calculations showed that, at most, two water molecules can hydrogen bond with the oxygen atom of the nitroxyl group of Tempo, and that a single water molecule forms a hydrogen bond that is ca. 30% stronger than the H_2O-H_2O hydrogen bond. These calculations led to a postulate that Tempo diffuses along the interface largely unimmersed, and that it is coupled to the interfacial water via hydrogen bonding with H_2O. In view of this postulate, the viscosity of the aqueous liquid/vapor interfacial region obtained by interpreting the Tempo diffusion constant in the low concentration region is as much as 4 times smaller than that of bulk liquid water.

Introduction

The importance of the aqueous liquid/vapor interface is difficult to overemphasize. Its properties are relevant to the atmospheric and environmental chemistry.[1−3] Many processes of practical importance occur at the aqueous interfaces, such as those in foams and emulsions.[4] Monolayer phenomena associated with this interface are used to model the behavior of biological membranes.[5,6] In recent years, advances in vibrational sum frequency spectroscopy,[7−11] X-ray reflectivity,[12,13] and EXAFS[14] revealed numerous structural details of the aqueous liquid/vapor interfacial region, such as its width, the extent of hydrogen bonding, and the orientational distribution of the water molecules. Our current understanding of the interfacial water is further broadened by the molecular dynamics calculations.[15−21] However, few of these investigations offer insight into the dynamic characteristics of aqueous interfaces. Thus, parameters such as the viscosity of water in the liquid/vapor interfacial region have not been, thus far, experimentally accessible. This report describes an experimental approach that offers such insight.

Our experimental approach involves 2D electrochemical measurements carried out with line microelectrodes positioned in the plane of the air/water interface.[22] Two-dimensional electrochemistry is used to characterize the lateral mobility of 2,2,6,6-tetramethyl-1-piperidynyloxy (Tempo) on the water surface in equilibrium with low concentrations of Tempo in the

(1) Seinfeld, J. H.; Pandis, S. N. *Atmospheric Chemistry and Physics*, Wiley: New York, 1998.
(2) Finlayson-Pitts, B. J.; Pitts, J. N., Jr. *Chemistry of the Upper and Lower Atmosphere*; Academic Press: San Diego, CA, 2000.
(3) Kolb, C. E. *Nature* **2002**, *417*, 597−598.
(4) Dukhin, S. S.; Kretzschmar, G.; Miller, R. *Dynamics of Adsorption at Liquid Interfaces: Theory, Experiment, Application*; Elsevier: Amsterdam, 1995.
(5) Cadenhead, D. A. In *Structure and Properties of Cell Membranes: Methodology and Properties of Membranes*; Benga, G., Ed.; CRC Press: Boca Raton, FL, 1985; Vol. 3, pp 21−62.
(6) Lipowsky, R.; Sackmann, E. *Structure and Dynamics of Membranes*; Elsevier: Amsterdam, 1995; Vols. 1A and 1B.
(7) Richmond, G. L. *Chem. Rev.* **2002**, *102*, 2693−2724.
(8) Richmond, G. L. *Annu. Rev. Phys. Chem.* **2001**, *52*, 357−389.
(9) Allen, H. C.; Raymond, E. A.; Richmond, G. L. *Curr. Opin. Colloid Interface Sci.* **2000**, *5*, 74−80.
(10) Miranda, P. B.; Shen, Y. R. *J. Phys. Chem. B* **1999**, *103*, 3292−3307.
(11) Eisenthal, K. B. *Chem. Rev.* **1996**, *96*, 1343−1360.
(12) Braslau, A.; Pershan, P. S.; Swislow, G.; Ocko, B. M.; Als-Nielsen, J. *Phys. Rev. A* **1988**, *38*, 2457.
(13) Braslau, A.; Deutsch, M.; Pershan, P. S.; Weiss, A. H. *Phys. Rev. Lett.* **1985**, *54*, 114−117.
(14) Wilson, K. R.; Schaller, R. D.; Co, D. T.; Saykally, R. J.; Rude, B. S.; Catalano, T.; Bozek, J. D. *J. Chem. Phys.* **2002**, *117*, 7738−7744.
(15) Maroncelli, M.; Fleming, G. R. *J. Chem. Phys.* **1988**, *89*, 5044−5069.
(16) Townsend, R. M.; Rice, S. A. *J. Chem. Phys.* **1991**, *94*, 2207−2218.
(17) Pohorille, A.; Wilson, M. A. Viewpoint 9: Molecular Structure of Aqueous Interfaces. *J. Mol. Struct. (THEOCHEM)* **1993**, *284*, 271−298.
(18) Benjamin, I. *Phys. Rev. Lett.* **1994**, *73*, 2083.
(19) Taylor, R. S.; Dang, L. X.; Garrett, B. C. *J. Phys. Chem.* **1996**, *100*, 11720−11725.
(20) Dang, L. X.; Chang, T.-M. *J. Chem. Phys.* **1997**, *106*, 8149.
(21) Sokhan, V. P.; Tildesley, D. J. *Mol. Phys.* **1997**, *92*, 625−640.
(22) Majda, M. In *Thin Films, Organic Thin Films and Surfaces: Directions for the Nineties*; Ulman, A., Ed.; Academic Press: New York, 1995; Vol. 20, pp 331−347.

10.1021/ja042969j CCC: $30.25

bulk. The molecular structure of Tempo, a reversible redox probe,[23,24] is shown below.

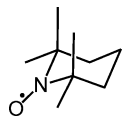

We rely on slow scan 2D voltammetry to first measure the total current due to the sum of the diffusion-limited transport of Tempo along the water surface (the 2D component) and in the bulk of electrolyte (the 3D component). We next measure the bulk (3D) component of the diffusion-controlled current with the same line electrode, after the water surface is covered with a stearic acid monolayer. This prevents Tempo from partitioning to the air/water interface and eliminates the surface component of the voltammetric current. The difference between the total current and the current due to the bulk transport is then interpreted in terms of the Tempo lateral diffusion constant on the water surface.[25] These measurements and the electronic structure calculations of the extent of Tempo−water interactions reveal that the viscosity of the air/water interfacial region is as much as 4 times lower than the viscosity of bulk water.

Experimental Section

Materials. 2,2,6,6-Tetramethyl-1-piperidynyloxy (Tempo) (98% Aldrich) was purified by sublimation. 4-Hydroxy-Tempo (Aldrich) was purified by column chromatography. Octadecyltrichlorosilane (OTS) and 3-mercaptopropyltrimethoxysilane (MPS) were from Aldrich. OTS was vacuum-distilled into glass ampules, which were sealed immediately afterward. They were opened as needed immediately prior to the individual experiments. Octadecylmercaptan (OM) (Tokyo Kadei, Tokyo, Japan) was used without further purification. Reagent-grade 70% $HClO_4$ (Fisher, ACS-certified), $LiClO_4$ (99.99%, Aldrich), and all other chemicals were used as received without further purification. House-distilled H_2O was passed through a four-cartridge Millipore purification train and a 0.2 μm hollow-fiber final filter. The resistivity of the resulting water (DI water) was 18.3 MΩ cm.

Fabrication of the Line Electrodes. Two-dimensional electrochemical measurements at the air/water interface required "line" microelectrodes, which are held just above the interface touching the water surface, and which self-position to become exactly aligned with the plane of the air/water interface.[22,26,27] They were produced by creating a sharp gradient of wettability along a fracture line of 100 nm thick gold films, vapor-deposited on microscope glass slides (ca. 8 × 20 mm^2), and subsequently coated with monolayer films of OM and OTS. The fabrication of these electrodes was previously described in detail.[27]

Electrochemical Measurements. All cyclic voltammetric experiments were done with a CH Instruments Model 660B electrochemical analyzer (Austin, TX) in a three-electrode setup with an SCE reference electrode and a Pt counter electrode at 21 °C. To obtain the voltammograms due to the lateral diffusion of Tempo on the water surface, a line electrode was placed on the surface of a Tempo solution also containing 50 mM $LiClO_4$ and 1 mM $HClO_4$ to record cyclic voltammograms due to both the surface and the bulk population of Tempo. After this experiment, the surface of the Tempo solution was covered with a monolayer film of stearic acid. The film was spread from a chloroform solution using a quantity 30% in excess of the monolayer coverage. The same line electrode was then placed again on the stearic acid-covered water surface to record additional cyclic voltammograms due to the bulk population of Tempo. Using nonamphiphilic 4-hydroxy-Tempo, we determined that the presence of a stearic acid monolayer on the water surface does not interfere with the recording of the bulk population of Tempo. In those experiments carried out using 4-hydroxy-Tempo concentrations from 0.1 to 1 mM, the voltammetric current due to the oxidation of 4-hydroxy-Tempo was the same regardless whether a line electrode was placed on the clean or on the stearic acid-covered water surface. A copper Faraday cage was used in all electrochemical experiments to minimize noise.

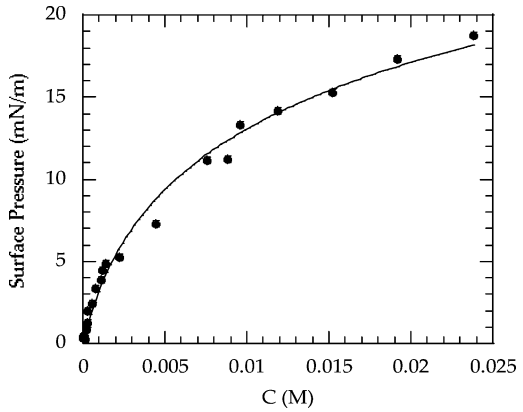

Figure 1. Tempo partitioning isotherm. See eqs 1−3 and the related discussion. The data points are averages of 5−8 individual, repetitive measurements, and the error bars (equal in size to the diameter of the data points) represent standard deviations of ±0.2 mN/m. The line represents best fit to the data points obtained using a nonlinear least-squares method.

Surface Tension Measurements. Surface tension measurements of the Tempo solutions were done with a DuNouy tensiometer (model 70535, CSC Scientific Co. Inc.). The tensiometer's Pt ring was cleaned in a Bunsen burner flame between each measurement to increase the precision and reproducibility of these measurements.

Electronic Structure Calculations. A series of calculations were performed on an isolated Tempo, a Tempo coordinated to small numbers of water molecules, and small isolated water clusters to predict the strength of hydrogen bonding between Tempo and such clusters. Geometries were optimized using the unrestricted Hartree−Fock (UHF) method with the standard 6-31G* basis set.[28] No significant spin contamination was found in the UHF wave functions. Final single point energies at these optimized geometries were then evaluated, including the effect of electron correlation via unrestricted second-order Møller−Plesset theory with core orbitals frozen, using the 6-31+G* basis. This level of theory, which may be denoted as UMP2(fc)/6-31+G*//UHF/6-31G*, is believed to be sufficient to characterize trends in the binding energies as a function of the number of coordinated water molecules. All calculations were performed using the Q-Chem program.[29]

Results and Discussion

We first discuss the measurements of the Tempo partitioning constant (K). These were done by the classical surface tension method using a ring tensiometer. The results are shown in Figure 1. They were interpreted in terms of the Langmuir−Szyszkowski

(23) Krzyczmonik, P. H. S. *J. Electroanal. Chem.* **1992**, *335*, 233−251.
(24) Baur, J. E.; Wang, S.; Brandt, M. C. *Anal. Chem.* **1996**, *68*, 3815−3821.
(25) Malec, A. D.; Wu, D. G.; Louie, M.; Skolimowski, J. J.; Majda, M. *Langmuir* **2004**, *20*, 1305−1310.
(26) Johnson, M. J.; Anvar, D. J.; Skolimowski, J. J.; Majda, M. *J. Phys. Chem. B* **2001**, *105*, 514−519.
(27) Johnson, M. J.; Majmudar, C.; Skolimowski, J. J.; Majda, M. *J. Phys. Chem. B* **2001**, *105*, 9002−9010.
(28) Jensen, F. *Introduction to Computational Chemistry*; Wiley: Chichester, U.K., 1999.
(29) Kong, J.; White, C. A.; Krylov, A. I.; Sherrill, D.; Adamson, R. D.; Furlani, T. R.; Lee, M. S.; Lee, A. M.; Gwaltney, S. R.; Adams, T. R.; Ochsenfeld, C.; Gilbert, A. T. B.; Kedziora, G. S.; Rassolov, V. A.; Maurice, D. R.; Nair, N.; Shao, Y. H.; Besley, N. A.; Maslen, P. E.; Dombroski, J. P.; Daschel, H.; Zhang, W. M.; Korambath, P. P.; Baker, J.; Byrd, E. F. C.; Van Voorhis, T.; Oumi, M.; Hirata, S.; Hsu, C. P.; Ishikawa, N.; Florian, J.; Warshel, A.; Johnson, B. G.; Gill, P. M. W.; Head-Gordon, M.; Pople, J. A. *J. Comput. Chem.* **2000**, *21*, 1532−1548.

isotherm equation describing the relationship between the surface pressure of a surfactant at the air/water interface, π and its bulk concentration, C:

$$\pi = RT\Gamma_{max} \ln(1 + KC) \quad (1)$$

where Γ_{max} is the surface concentration of the surfactant corresponding to full monolayer coverage, and K is the partition constant.[4] The Langmuir−Szyszkowski isotherm combines the well-known Gibbs adsorption isotherm, relating surface tension (γ) to the surfactant's bulk concentration (C)

$$\Gamma = -\frac{1}{RT}\frac{d\gamma}{d\ln C} \quad (2)$$

and the Langmuir isotherms, which relates surface excess of the surfactant (Γ) to the partition constant (K):

$$\Gamma = \Gamma_{max}\frac{KC}{1 + KC} \quad (3)$$

With the knowledge that the surface pressure is defined as the difference between water surface tension in the absence and in the presence of the adsorbed molecules, $\pi = \gamma_0 - \gamma$, eq 1 allows us to directly relate the measured surface tension to the Tempo's bulk concentration. By fitting eq 1 to the data in Figure 1, we obtained $K = 640 \pm 99$ M^{-1} and $\Gamma_{max} = (2.7 \pm 0.2) \times 10^{-10}$ mol/cm^2 and the correlation coefficient, $R = 0.995$. The value of Γ_{max} corresponds to a mean molecular area of 62 Å^2/molecule. The latter reflects reasonably well the projected size of a Tempo molecule. We note also that the Tempo partition constant is over 1 order of magnitude smaller than 2.3×10^4 M^{-1} that we recently obtained for a 4-octaneamide derivative of Tempo (C_8Tempo) shown below.[25]

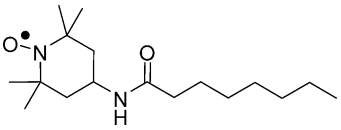

This ratio of the partition constants reflects the structural differences and the expected stronger amphiphilic character of C_8Tempo relative to that of Tempo.

To measure the lateral mobility of Tempo along the air/water interface, two sets of electrochemical measurements were carried out. In the first set of experiments, a line electrode was positioned on the water surface (Tempo solutions of different concentrations in pH 3.0, 50 mM $LiClO_4$ electrolyte) and a slow scan voltammogram was recorded. In these measurements, the voltammetric current is a sum of the diffusion-controlled contributions due to the Tempo populations in the bulk of the electrolyte and on the water surface. As outlined in the Experimental Section, our line microelectrodes consist of a 100 nm gold microband contacting the bulk of the electrolyte solution. The edge of the microband is aligned with the plane of the air/water interface where it probes the Tempo molecules partitioned to and diffusing along the water surface. In the second set of the voltammetric experiments done with the same line microelectrodes, the surface of the Tempo solution in the trough was covered with a monolayer film of stearic acid. We showed previously that this prevents partitioning of surfactants to the air/water interface but does not interfere with the recording of the current due to the bulk population of the surfactant.[25]

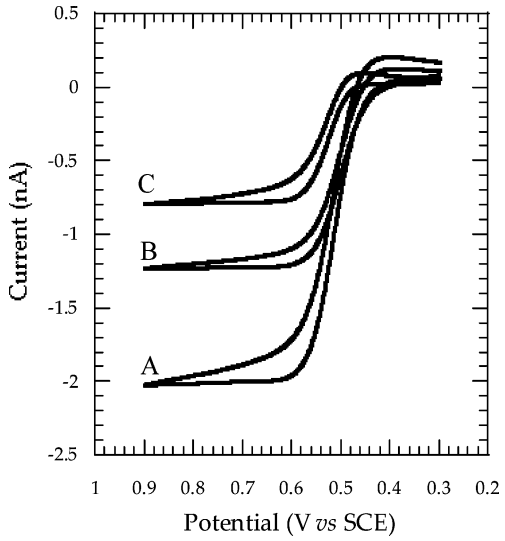

Figure 2. Cyclic voltammograms recorded with a 590 μm line electrode positioned on the surface of a 0.10 mM Tempo, 50 mM $LiClO_4$, 1.0 mM $HClO_4$ solution. (A) clean surface experiment; (B) surface is covered with a monolayer of stearic acid; (C) difference of curve A and curve B. Scan rate, 20 mV/s, $T = 21$ °C.

Typical results of both experiments are shown in Figure 2. In that figure, trace C was obtained by subtracting the bulk current (trace B) from the total current (trace A). Trace C, referred to as surface voltammogram, represents the surface population of Tempo and was used to obtain its lateral diffusion constant, D_s. We used the same approach to measure the lateral mobility of C_8Tempo at the air/water interface.[25] However, we note that this approach is rigorously correct only in cases in which there is no coupling between the bulk and surface populations of the surfactant. This point is further discussed in the Concluding Remarks section of this report.

Two features of the surface voltammograms are worth noting. First, they contain only a very small cathodic branch due to the reduction of Tempo's oxonium cation, Tempo$^+$. This is understandable since the latter is more water soluble and desorbs from the air/water interface on the time scale of these experiments. The second feature is the dependence of the shape of the surface voltammograms on the length of the line electrodes. This is shown in Figure 3, where surface voltammograms recorded with the 590 μm, 4.0 mm, and 10 mm electrodes are shown. The one recorded with a 590 μm line electrode is sigmoidal, while the anodic current recorded with the longer electrodes features a peak. This difference suggests a greater contribution of a 2D radial (hemicircular) diffusion component in the cases of the measurements done with the shortest line electrode.[30] In other words, on this time scale, the diffusion layer thickness developed in the plane of the air/water interface is comparable to, or greater than, ca. 590 μm.

Considering this analysis, to extract Tempo's lateral diffusion constant (D_s), we relied on the equation derived by Aoki et al. for the case of linear sweep voltammetry at microcylinder electrodes.[31] It applies, as in our experiment, to mixed linear and hemicylindrical diffusion control cases. The necessary 3D → 2D reduction of dimensionality involved a substitution of

(30) Bard, A. J.; Faulkner, L. R. *Electrochemical Methods: Fundamentals and Applications*, 2nd ed.; J. Wiley & Sons: New York, 2001.
(31) Aoki, K.; Honda, K.; Tokuda, K.; Matsuda, H. *J. Electroanal. Chem.* **1985**, *182* (2), 267−279.

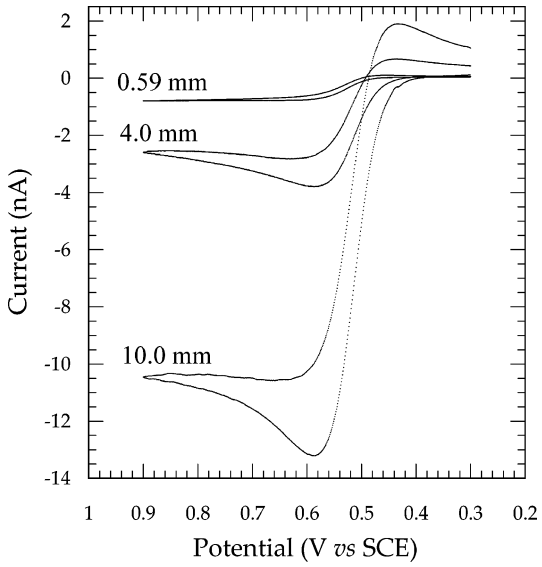

Figure 3. Comparison of three "difference" voltammograms obtained with the line electrodes of different length marked in the figure. The experimental conditions are as those in Figure 2.

the product of the cylinder length and the bulk concentration (C) by the surface concentration (Γ), as described previously.[25,32] In other words, to describe the behavior of a line electrode in 2D, we must use microband electrode equations in which the reduction of dimensionality removes the length of the band in the voltammetric current equation. We also relied on a well-established approximation stating that, in the limit of long times, current at a microband electrode with width w can be well approximated by current at a hemicylindrical electrode of radius r when one makes a substitution, $r = w/4$.[33] These substitutions yielded the following (at 293 K):

$$i_p = (2.13 \times 10^5)\Gamma w D^{1/2} v^{1/2} + (1.09 \times 10^5)\Gamma w^{0.15} D^{0.925} v^{0.075} \quad (4)$$

We note that the width, w, represents the length of our line microelectrode, as explained earlier. The resulting plot of Tempo D_s versus the mean molecular area (MMA) is shown in Figure 4.

Considering the data in Figure 4, we can distinguish two qualitatively different regions. At higher surface concentrations of Tempo (MMA < 350 Å^2/molecule), the D_s values tend to be high and are subject to considerable scatter. This region corresponds to the surface pressure decreasing from ca. 5 mN/m at 100 Å^2/molecule to 0.5 mN/m at 350 Å^2/molecule. It is, therefore, plausible that the observed high values of D_s and the data scatter in this region are due to the convective transport of Tempo induced by the surface pressure gradient in the monolayer films. The latter is created by Tempo electro-oxidation and desorption. This phenomenon, often referred to as Marangoni flow, has been described in the literature.[34−36] In the

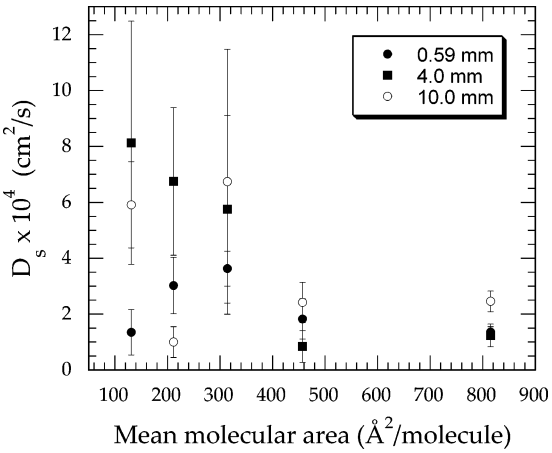

Figure 4. Plot of the measured lateral diffusion constant of Tempo at the air/water interface as a function of Tempo MMA. The symbols correspond to the length of the line microelectrodes used in the measurements (see Figure 3). The error bars represent the standard deviations obtained on the basis of three measurements recorded with each of three different line electrodes of a given length.

region of lower surface concentrations (MMA > 400 Å^2/molecule), the surface pressure further decreases and can be estimated to be less than 0.3 mN/m. Furthermore, the D_s values become independent of the Tempo surface concentration and are no longer subject to large scatter as in the region of MMA < 350 Å^2/molecule. They also become independent of the electrode length. These facts allow us to conclude that surface convection no longer plays a significant role in influencing the magnitude of D_s, and that the latter is largely determined by the lateral diffusion of Tempo along the interface. We will next deal with the interpretation of the average D_s value in that region of $(1.5 \pm 0.7) \times 10^{-4}$ cm^2/s.

First of all, it is fair to say that a diffusion constant of 1.5×10^{-4} cm^2/s is unusually high for any species in aqueous systems, with the exception of protons. The aqueous diffusion constants of H_2O and NO, to mention two molecules considerably smaller than Tempo, are nearly 1 order of magnitude smaller, 2.3×10^{-5} and 2.6×10^{-5} cm^2/s,[37] respectively. Interpretation of our own measurements of the current due to the Tempo diffusion in bulk water (Figure 2 trace B) yields $D_b = (8.7 \pm 0.8) \times 10^{-6}$ cm^2/s. However, our earlier measurements of the lateral mobility of C_nTempo amide surfactants, with n in the range of 8−18, yielded D values between 1.0 and 1.5×10^{-5} cm^2/s at MMAs between 400 and 800 Å^2/molecule, respectively.[25] These relatively high D values were related to the shallow immersion depth of the Tempo surfactants. Recent X-ray reflectivity measurements carried out for C_{18}Tempo amide showed that its orientation on the water surface favors immersion of the amide group in the subphase.[38] Both the piperidine ring and the alkane chain are positioned above the water surface. Clearly, to understand the high D_s of Tempo in the plateau region of Figure 4, we must first understand the extent of Tempo−water interactions at the air/water interface.

To this end, consider the structure of Tempo in Figure 5A obtained on the basis of the published X-ray crystallographic

(32) Charych, D. H.; Goss, C. A.; Majda, M. *J. Electroanal. Chem.* **1992**, *323*, 339−345.
(33) Szabo, A.; Cope, D. K.; Tallman, D. E.; Kovach, P. M.; Wightman, R. M. *J. Electroanal. Chem.* **1987**, *217*, 417−423.
(34) Gallardo, B. S.; Gupta, V. K.; Eagerton, F. D.; Jong, L. I.; Craig, V. S.; Shah, R. R.; Abbott, N. L. *Science* **1999**, *283*, 57−60.
(35) Gallardo, B. S.; Metcalfe, K. L.; Abbott, N. L. *Langmuir* **1996**, *12*, 4116−4124.
(36) Bennett, D. E.; Gallardo, B. S.; Abbott, N. L. *J. Am. Chem. Soc.* **1996**, *118*, 6499−6505.
(37) Malinski, T.; Taha, Z.; Grunfeld, S. *Biochem. Biophys. Res. Commun.* **1993**, *193*, 1076−1082.
(38) Wu, D. G.; Malec, A. D.; Majewski, J.; Majda, M. *Electrochim. Acta*, submitted for publication December 2004.

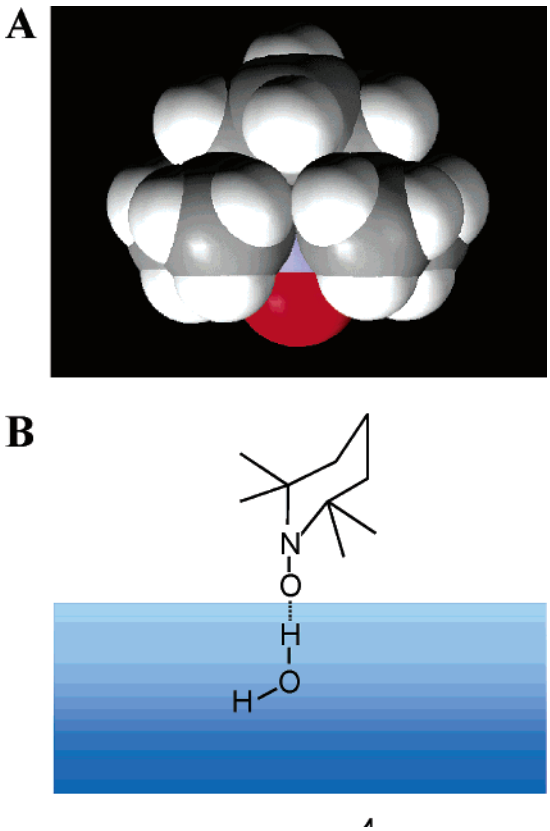

Figure 5. (A) Space filling structure of Tempo.[39] (B) Drawing of Tempo positioned above the air/water interface and coupled to the interfacial region via a H_2O molecule hydrogen bonded to its nitroxide group.

data.[39] Tempo is viewed in the direction perpendicular to the boatlike piperidine ring. This projection enables one to recognize the extent to which the two pairs of methyl groups attached to the two carbon atoms adjacent to the nitrogen shield the nitroxy group, Tempo's polar fragment. This realization makes us postulate that the presence of the four methyl groups next to the nitroxide constrains Tempo's ability to be immersed in the water when it partitions to the air/water interface. This postulate is supported by the molecular dynamics calculations of single, small, nonionic molecules, such as phenol,[40] *p-n*-pentylphenol,[41] methanol, and ethanol,[42] at the air/water interface by Pohorille and co-workers. They showed that the immersion depth of these molecules is essentially limited to their hydroxyl group. Specifically, in all these cases, the average position of the carbon atom linked to the oxygen of the hydroxyl group was 0.5−1 Å above the Gibbs dividing surface. The latter is the plane in the aqueous interfacial region marking the water density equal to 50% of the bulk value. According to several molecular dynamics calculations, the 10−90% thickness of the water interfacial region (the width over which the density of water changes from 10 to 90% of its bulk liquid value) is approximately 3.5 Å.[16,17,19,21] Considering these theoretical results, it is, indeed, plausible to envision the location of Tempo to be just above the Gibbs surface. With this in mind, the following two scenarios concerning the extent of Tempo−water interactions can be considered in order to understand our measured D_s values.

The first limiting case assumes negligible Tempo−water interactions. If this were true, we would expect Tempo to diffuse on the water surface with a diffusion constant limited only by the rate of the mutual intermolecular collisions. That diffusion constant can be obtained using the Enskog theory of dense gases extended by Alder to liquid densities on the basis of his molecular dynamics calculations.[43,44] It predicts that the diffusivity of hard-sphere liquids (D_{HS}) can be expressed by the following equation:

$$D_{HS} = \frac{\sigma}{4}\left(\frac{\pi RT}{m}\right)^{1/2}(Z-1)^{-1}\frac{D_{HS}}{D_E} \qquad (5)$$

where σ is the molecular diameter; m is molecular mass, and Z is the compressibility factor ($Z = PV/RT$). For the hard-sphere liquids, Z can be related to the relative volume of the fluid, V/V_0 (V is the actual volume of the fluid, and V_0 is the volume occupied by hard spheres when they are close packed). The term D_{HS}/D_E is the correction of the Enskog diffusion constant (D_E) obtained by Alder et al. as a function of V/V_0, by their molecular dynamics calculations.[44] While this theory treats the 3D case of hard-sphere liquids, we have successfully used it to account for the dependence of the lateral diffusion constant on the surface concentration observed for a number of amphiphilic ferrocene derivatives.[45] When applied to the present case of Tempo diffusion on the water surface under the assumption of negligible interactions with the water, we obtained, as previously,[45] a linearly increasing diffusion constant with the values of 1.2×10^{-3} and 2.2×10^{-3} for the two MMAs of 460 and 820 Å^2/molecule, respectively, in the plateau region of Figure 4. Since these D_{HD} values far exceed our measured D_s, and because the Enskog−Alder theory predicts increasing diffusivities with decreasing hard-sphere densities, this theory does not reflect the observed behavior of Tempo. These substantial discrepancies clearly suggest that Tempo−water interactions are not negligible.

The second, and a more realistic scenario, is to postulate, as shown schematically in Figure 5B, that Tempo is capable of forming a hydrogen bond with the water molecules in the aqueous interfacial region. Indeed, strong hydrogen bonding of the Tempo nitroxyl with the hydroxylic solvents has been determined to exist spectroscopically.[46,47] To test this hypothesis, we calculated the binding energies and molecular structures of isolated Tempo−H_2O clusters with an increasing number of water molecules. The binding energies of $(H_2O)_n$ clusters were also obtained as a reference system. These data are listed in Table 1.

The following two conclusions are the most relevant to our measurements. First, Tempo can hydrogen bond with, at most, two water molecules. Clusters of Tempo with three and four water molecules involve only two hydrogen bonds with Tempo. See, for example, the calculated structure of the Tempo−$(H_2O)_4$ cluster in Figure 6. Second, a single water molecule binds to Tempo more strongly than it does to another water molecule

(39) Capiomony, A.; Lajzerowicz, J.; Legrand, J.-F.; Zeyen, C. *Acta Crystallogr.* **1981**, *B37*, 1557−1560.
(40) Pohorille, A.; Benjamin, I. *J. Chem. Phys.* **1991**, *94*, 5599−5605.
(41) Pohorille, A.; Benjamin, I. *J. Phys. Chem.* **1993**, *97*, 2664−2670.
(42) Wilson, M. A.; Pohorille, A. *J. Phys. Chem. B* **1997**, *101*, 3130−3135.
(43) Tyrrell, H. J. V.; Harris, K. R. *Diffusion in Liquids, A Theoretical and Experimental Study*; Butterworth: London, 1984, Vol. 5, p 266.
(44) Alder, B. J.; Gass, D. M.; Wainwright, T. E. *J. Chem. Phys.* **1970**, *53*, 3813−3826.
(45) Kang, Y. S.; Majda, M. *J. Phys. Chem. B* **2000**, *104*, 2082−2089.
(46) Mukerjee, P.; Ramachandran, C.; Pyter, R. A. *J. Phys. Chem.* **1982**, *86*, 3189−3197.
(47) Symons, M. C. A.; Pena-Nunez, A. S. *J. Chem. Soc., Faraday Trans. 1*, **1985**, *81*, 2421−2435.

Table 1. Binding Energies (kcal/mol) of Tempo and Water Clusters[a]

molecular cluster	binding energy
Tempo−H_2O	8.682
Tempo−$(H_2O)_2$	17.813
Tempo−$(H_2O)_3$	30.082
$(H_2O)_2$	6.815
$(H_2O)_3$	19.766
$(H_2O)_4$	33.658

[a] See Experimental Section.

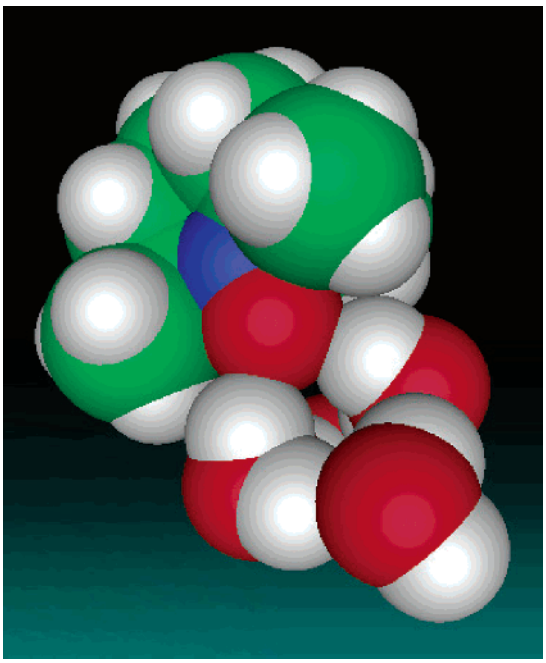

Figure 6. Structure of the Tempo−$(H_2O)_4$ cluster.

(see entries 1 and 4 in Table 1). We find also that the binding energy of the Tempo with two water molecules is smaller than that of the isolated water trimer, reflecting the stearically strained and thus weaker H_2O-H_2O interactions in Tempo−$(H_2O)_2$. A similar conclusion can be made by comparing the binding energies of Tempo−$(H_2O)_3$ and $(H_2O)_4$. Overall, the results of these calculations support our hypothesis of Tempo−water interactions schematically outlined in Figure 5B. Naturally, these calculations do not answer our next question concerning the dynamics of Tempo−water interactions. Specifically, it is not possible to say with certainty what the time-averaged size is of the Tempo−water cluster diffusing along the interface. The answer to this and related questions will likely emerge from molecular dynamics calculations. In the absence of those results, the binding energies in Table 1 lead us to estimate that, on average, Tempo is coupled to the aqueous interfacial region by one H_2O molecule hydrogen bonded to its nitroxyl oxygen. Consequently, we can interpret the average D_s value of 1.5×10^{-4} cm^2/s in terms of the apparent, long-term viscosity of the aqueous interfacial region, η_{int}. Recognizing the 2D nature of the D_s measurements, we recall that ${}^{3D}D = {}^{2}/_{3}\,{}^{2D}D$. Then, using the well-known Stokes equation, we find η_{int} to be 4 times smaller than that of the bulk water viscosity.

This estimate of the interfacial water viscosity is high relative to the molecular dynamics calculations offering the ratios of the water self-diffusion constant in the interfacial region to that in the bulk. Specifically, reorientation of the interfacial water molecules was found to be 5−40% faster than that of the bulk water by Maroncelli and Fleming.[15] Both Townsend and Rice[16] and Garrett and co-workers[19] reported the diffusion constant of water in the interfacial region to be greater than that in the bulk by 58 and 69%, respectively. This comparison may suggest that Tempo, regardless of the details of its hydrogen bonding, spends a fraction of the time diffusing along the interface not coupled to the interfacial region. Alternatively, this apparent discrepancy may suggest that the single H_2O molecule hydrogen bonded to Tempo samples, on average, the less viscous, vapor phase side of the interfacial region. We point out that the measured 10−90% thickness of the interfacial region that combines both the intrinsic density profile and the capillary wave contribution was reported to be 6.7 Å (ellipsometry)[48] and 6.8−8.0 Å (X-ray measurements).[12,49] These are substantially greater values than ca. 3.5 Å that is often reported as the 10−90% thickness by the molecular dynamics simulations.[16−19,21] Clearly, a more precise interpretation of our measurements must await additional molecular insights concerning the structure and dynamics of the Tempo−water interactions at the interface.

Concluding Remarks

In summary, our conclusions concerning the magnitude of Tempo D_s value and the interfacial water viscosity are approximate for a number of reasons. First, the measurements of D_s involved the voltammetric current subtraction method of Figure 2, which is rigorously correct only in the absence of coupling between the bulk and surface transport of Tempo to the line electrode. This approach introduces a positive error in D_s calculations if the kinetics of Tempo partitioning is fast. Since data concerning the rate of Tempo partitioning are not available to us, we work to include 4-alkane-Tempo derivatives that we expect will exhibit larger partition constants and thus minimize the importance of the bulk diffusion in the experiments of Figure 2. Furthermore, the fact that the measurements were done at the relatively high surface densities of Tempo on the water surface introduces a negative error in D_s. In other words, diffusion of the Tempo−water cluster is slowed by the intermolecular collisions of Tempo. In the limit of low concentrations, the problem has a solution in the form of Einstein's equation: $\mu^* = \mu(1 + 2.5\alpha)$, where μ^* and μ are the viscosities of a suspension and of an ambient fluid, respectively, and α is the concentration of particles by volume.[50,51] It applies for $\alpha \leq 0.02$.[50,51] Clearly, our system exceeds that limit. At ~600 $Å^2$/molecule, the average concentration in the plateau region of Figure 4, $\alpha = 0.10$. More importantly, our treatment of the interfacial water as a viscous continuum is a large simplification. This, however, is consistent with the long-time nature of the electrochemical measurements. Finally, the largest uncertainty is likely introduced by the assumption that the diffusion of Tempo is coupled to the diffusion of a single H_2O molecule immersed in the interfacial region.

These uncertainties notwithstanding, our original hypotheses that Tempo diffuses along the interface largely unimmersed and that it is coupled to the interfacial water via hydrogen bonding

(48) Beaglehole, D. *J. Phys. Chem.* **1987**, *91*, 5091−5092.
(49) Schwartz, D. K.; Schlossman, M. L.; Kawamoto, E. H.; Kellogg, G. J.; Pershan, P. S.; Ocko, B. M. *Phys. Rev. A* **1990**, *41*, 5687−5690.
(50) Happel, J.; Brenner, H. *Low Reynolds Number Hydrodynamics with Special Applications to Particulate Media*; Prentice Hall: Englewood Cliffs, NJ, 1965; Chapter 9, pp 431−473.
(51) Ladd, A. J. C. *J. Chem. Phys.* **1990**, *93*, 3484−3494.

with H_2O in the interfacial region are well supported by the electronic structure calculations. This behavior of Tempo is unique and substantially different than the behavior of 4-alkaneamide Tempo derivatives mentioned above and discussed in our previous reports.[25−27,38] The structure of those compounds features two polar fragments located on the opposite ends of the piperidine ring (see the structure of C_8Tempo above). Using X-ray reflectivity, we showed that the orientation of these C_n-Tempo amphiphiles favors interactions of the amide group with the aqueous subphase rather than that of the nitroxide moiety.[38] In view of the high polarity of the amide group, and knowing that, unlike the nitroxide, it is not shielded by the neighboring hydrocarbon fragments, it is easy to postulate a complete immersion of the amide group in the subphase.[25] Considering the size of this group and its capability to hydrogen bond with water, it is not surprising that the interfacial diffusion constants of the C_nTempo derivatives are independent of the chain length and that they are 1 order of magnitude lower than that of Tempo. The chain length independence is consistent with the amide immersion in the water, which limits the lateral mobility of these molecules in the low surface concentration region.[25] The unique behavior of Tempo reported above derives from the fact that the nitroxide is its only polar fragment, and that it is shielded by the four adjacent methyl groups. The latter limits its interactions with water, as we showed schematically in Figure 5b. This, together with the redox and ESR activity of Tempo, makes this molecule a uniquely valuable probe of the interfacial water dynamics.

Acknowledgment. We acknowledge the donors of the Petroleum Research Fund, administered by the American Chemical Society, for partial support of this research. Additional support was provided by the National Science Foundation through Grants CHE-0416349 to M.M. and CHE-9981997 to M.H.-G.

JA042969J